

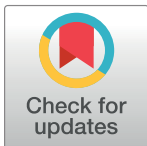
RESEARCH ARTICLE

Synthesis of a novel glucose capped gold nanoparticle as a better theranostic candidate

Saritha Suvarna¹, Ujjal Das², Sunil KC¹, Snehasis Mishra³, Mathummal Sudarshan⁴, Krishna Das Saha³, Sanjit Dey², Anindita Chakraborty⁴, Y. Narayana^{1*}

1 Department of Studies in Physics, Mangalore University, Mangalagangothri, Karnataka, India, **2** Department of Physiology, Centre for Nanoscience and Nanotechnology and Centre with Potential for Excellence in Particular Area (CPEPA), University of Calcutta, Kolkata, West Bengal, India, **3** Cancer Biology & Inflammatory Disorder Division, IICB, Kolkata, West Bengal, India, **4** UGC-DAE Consortium for Scientific Research Centre, Kolkata, West Bengal, India

* narayanay@yahoo.com



Abstract

Gold nanoparticles are predominantly used in diagnostics, therapeutics and biomedical applications. The present study has been designed to synthesize differently capped gold nanoparticles (AuNps) by a simple, one-step, room temperature procedure and to evaluate the potential of these AuNps for biomedical applications. The AuNps are capped with glucose, 2-deoxy-D-glucose (2DG) and citrate using different reducing agents. This is the first report of synthesis of 2DG-AuNp by the simple room temperature method. The synthesized gold nanoparticles are characterized with UV-Visible Spectroscopy, Fourier transform infrared spectroscopy (FTIR), Transmission electron microscopy (TEM) and selected area electron diffraction (SAED), Dynamic light scattering (DLS), and Energy-dispersive X-ray spectroscopy (SEM-EDS). Surface-enhanced Raman scattering (SERS) study of the synthesized AuNps shows increase in Raman signals up to 50 times using 2DG. 3-(4, 5-dimethylthiazol-2-yl)-2,5-diphenyl tetrazolium bromide (MTT) assay has been performed using all the three differently capped AuNps in different cell lines to assess cytotoxicity if any, of the nanoparticles. The study shows that 2DG-AuNps is a better candidate for theranostic application.

OPEN ACCESS

Citation: Suvarna S, Das U, KC S, Mishra S, Sudarshan M, Saha KD, et al. (2017) Synthesis of a novel glucose capped gold nanoparticle as a better theranostic candidate. PLoS ONE 12(6): e0178202. <https://doi.org/10.1371/journal.pone.0178202>

Editor: Yogendra Kumar Mishra, Institute of Materials Science, GERMANY

Received: October 12, 2016

Accepted: May 9, 2017

Published: June 5, 2017

Copyright: © 2017 Suvarna et al. This is an open access article distributed under the terms of the [Creative Commons Attribution License](https://creativecommons.org/licenses/by/4.0/), which permits unrestricted use, distribution, and reproduction in any medium, provided the original author and source are credited.

Data Availability Statement: All relevant data are available in the manuscript.

Funding: This work was supported by F. No. 41-877/2012/SR dated 26-07-2012.

Competing interests: The authors have declared that no competing interests exist.

Introduction

Application of nanotechnology has gained a major thrust in research especially in the area of medicine and biology. With several gold nanoparticle based therapies currently undergoing clinical trials, gold nanoparticles have become the subject of a wide ranging international research effort with preclinical studies underway [1]. Synthesis of nanoscale structures of inert metals like gold are of great interest for the present day researchers as gold possess certain physical properties which are suitable for several biomedical applications. Thus gold nanoparticles show significant future promise in the fields of diagnostic imaging and therapy, including multifunctional drug-delivery vehicles [2–8], The Au-ZnO nanocomposite exhibits significant enhancement in the Raman signals for C₇₀ C₇₀ molecules [9]. Various standard

protocols and recent advances for shape-controlled synthesis of nanocrystals are reported, it is clear that significant progress has been made towards design synthesis of nanocrystals, with desired shape, crystallinity and composition by controlling the nucleation and growth process using specific synthetic protocols [10]. Studies also reported doses (concentration) of Au-Nps required for controlling the growth or decay of C₂C₁₂ myoblast cells. The obtained results clearly demonstrate that the treatments with nanoparticles diminished the growth of cells. Apoptosis was determined to be enhanced with an increase in nanoparticle concentration, and a significant concentration of nanoparticles resulted in cellular death [11]. Additionally, the galvanic replacement reaction with HAuCl₄ in an organic medium was implemented to prepare hydrophobic hollow Au-Ag nanocages with tunable localized surface Plasmon resonances [12]. The superiority of atom beam sputtering over in beam mixing and ion implantation in the synthesis of Au nanoparticles has also been demonstrated. The possibility of using Au-SiO₂ nanocomposites as a biosensor for the detection of ovarian cancer cells has been explored [13]. Studies also lay special emphasis on the uniqueness of the gold nanoparticles for treatment of life threatening diseases like cancer [14]. Available reports show potential of gold nanoparticles in the field of photodynamic therapy due to their ability of producing heat to kill the tumors [15]. AuNPs are reported as good photo-thermal agents for cancer therapy because they show efficient local heating upon excitation of surface plasmon oscillations. The strong absorption, efficient heat conversion, high stability, inherent low toxicity and well-defined surface chemistry of AuNps, contribute to the growing interest in their photothermal therapy (PTT) applications [16]. In the recent past, researchers also discussed the near-infrared-active AuNps, which include different shape of nanoparticle systems, especially regarding the clinical translation of AuNp [17]. Variety of shapes have driven a new wave of interest in their optical properties and thus offers applications like imaging and spectroscopic detection of cancer [18,19] Urchin-shaped gold nanoparticles deserves special mention as this type of the AuNps may find applications as materials for Surface Enhanced Raman Scattering (SERS) [20]. The gold supraparticles have nanoparticle building blocks in close contact that generate highly intense SERS signals. They also generate plasmonic heat more efficiently and kill more cancer cells than the constituent nanoparticle building blocks. These traits make the proposed crystallographically aligned supraparticles promising candidates for nanomedicine applications such as SERS -based diagnostics and plasmonics-based theranostics [21]. Studies also reported generalized application of gold nanostars for ultrasensitive identification of molecules based on both localized surface Plasmon resonance (LSPR) and surface enhanced Raman scattering (SERS) are the requirements of plasmonic sensors, related to sufficiently large areas where nanoparticles are uniformly immobilized with high density, as well as mechanical flexibility, which offers additional advantages for real world applications [22]. However, although gold is biologically inert and thus shows much less toxicity as compared to other metal nanoparticles, gold has a relatively lower rate of clearance from circulation and hence can pose serious deleterious effects on health [23]. Recent studies showed that AuNPs can cross the blood-brain barrier, interact with the DNA and even produce genotoxic effects [24]. As such, surface modifications of AuNps are gaining attention in current day research programs where attaching a ligand and/or capping of the AuNps could help making the particles more biocompatible so as to achieve specific targeting of diseased cells and tissues [25,26]. Synthesizing AuNps with lesser toxicity is now one of the primary interests in the field of nanotechnology for its applicability in biomedical sciences. Based on this perspective, the present work has been designed to formulate a synthesis of a novel glucose capped gold nanoparticle which can be considered as a better theranostic candidate.

The glucose analog 2-deoxy-D-glucose (2DG), an inhibitor of glycolytic ATP production and glucose transport is the most widely reported, metabolic inhibitor for targeting glucose

metabolism. In addition, 2DG can induce oxidative stress [27], inhibits N-linked glycosylation and induces apoptosis via endoplasmic reticulum(ER) stress [28]. It can efficiently slow cell growth and potently facilitate apoptosis in specific cancer cells. Although 2DG itself has limited therapeutic effect in many types of cancers, it may be combined with other therapeutic agents or radiotherapy[29] to exhibit a synergistic anticancer effect [30]. Some earlier studies described the Warburg effect and discussed about 2DG and its underlying mechanisms as potential application for cancer treatment [31]. 2-deoxy-D-glucose labeled gold nanoparticles have been shown to provide high-resolution metabolic and anatomic information of tumor in a single CT scan [32,33]. The importance of computed tomography (CT) as one of the leading radiology techniques applied in the field of biomedical imaging escalated the development of nanoparticles as the next generation CT contrast agents [34–37]. Studies showed that glucose capped gold nanoparticles has been specially chosen to target cancer cells, as such capped nanoparticles show faster cellular uptake in cancer cells. Additionally, larger numbers of glucose molecules are internalized via glucose transporter (GLUT) receptors present on the cancer cell surface [38,39]. It is already established that brain tumor cells have over expression of the facilitative glucose transporter protein (GLUT) [40]. Recently 2-deoxy-D-glucose modified poly (ethylene glycol)-co-poly(trimethylene carbonate) nanoparticles (DGlu-Np) were developed as a potential dual-targeted drug delivery system for enhancing the blood brain barrier penetration via Glut-mediated transcytosis and improving the drug accumulation in the glioma via GLUT-mediated endocytosis [41]. Our present paper describes the synthesis of differently capped gold nanoparticles and characterization of the nanoparticles by different techniques. Idea of developing 2DG-capped AuNps is inspired by the classic citrate method and the greener glucose method for gold nanoparticle preparation. The primary motivation behind the work has been to develop a simple novel method of capping of AuNps and further to compare the citrate- and glucose-reducing gold nanoparticles with 2DG capped AuNps to determine the most potential candidate amongst these AuNps for biomedical applications. Evaluation of biocompatibility of the nanoparticles has been carried out using HeLa, HepG2 and HCT 116 cell lines.

Materials and methods

Materials

HAuCl₄·3H₂O (≥ 99.9%, Sigma Aldrich, USA), β-D-glucose (≥ 99.9%, Sigma Aldrich, USA), 2-deoxy-D-glucose (≥98% (GC), crystalline, Sigma Aldrich, USA), Sodium Hydroxide (NaOH), (Merck Chemicals) are used in the present study. HeLa (Cervical Carcinoma), HCT 116 (Human Colorectal Carcinoma) and Hep G2 (Human liver Carcinoma) Cell lines are purchased from NCCS, Pune, India and cultured in DMEM medium supplemented with 10% fetal bovine serum (FBS) and 1% antibiotic (PSN) at 37°C in a humidified atmosphere under 5% CO₂. After 75–80% confluency, cells, harvested with 0.025% trypsin and 0.52 mM EDTA in phosphate buffered saline(PBS), are seeded at required density to allow them to re-equilibrate a day before the start of experiment.

Methodology

Synthesis of Au-Nps. Synthesis of Gu-AuNPs: Glucose capped AuNPs are synthesized by chemical route using HAuCl₄ and β-D-Glucose as described by earlier researchers [42]. The aqueous solution of 0.05 M HAuCl₄·3H₂O is added to β-D-glucose (0.03 M) and stirred for 30 minutes. Subsequently, 0.5 M sodium hydroxide (NaOH) is added for completing reduction of gold salt. This resulted in a red colored solution of Glu-AuNps. β-D-glucose acted as reducing as well as capping agent in the AuNp synthesis.

Synthesis of 2-deoxy-D-glucose-AuNps: Synthesis of 2-deoxy-D-glucose capped gold nanoparticle has been done in our lab for the first time by a half an hour reaction at room temperature. The method briefly described as follows. We synthesized 2-deoxy-D-glucose capped gold nanoparticles by chemical route using HAuCl_4 and 2-deoxy-D-Glucose. The aqueous solution of 0.05 M $\text{HAuCl}_4 \cdot 3\text{H}_2\text{O}$ has been added to 2-deoxy-D-glucose (0.04 M) and stirred for 30 minutes. Subsequently, 0.5 M sodium hydroxide (NaOH) is added for completing reduction of gold salt. This resulted in a brisk red colored solution of 2DG-AuNps. 2-deoxy-D-glucose acted as reducing as well as capping agent in the AuNp synthesis as shown in Fig 1.

Capping has been confirmed using FTIR analysis. Chemical equation for the reaction is shown in Fig 2.

Synthesis of Citrate-AuNPs: Citrate- gold nanoparticles have been synthesized using chemical method. Conventional techniques for aqueous synthesis of gold nanoparticles involve reduction of Au(III)Cl_3 with trisodium citrate [43].

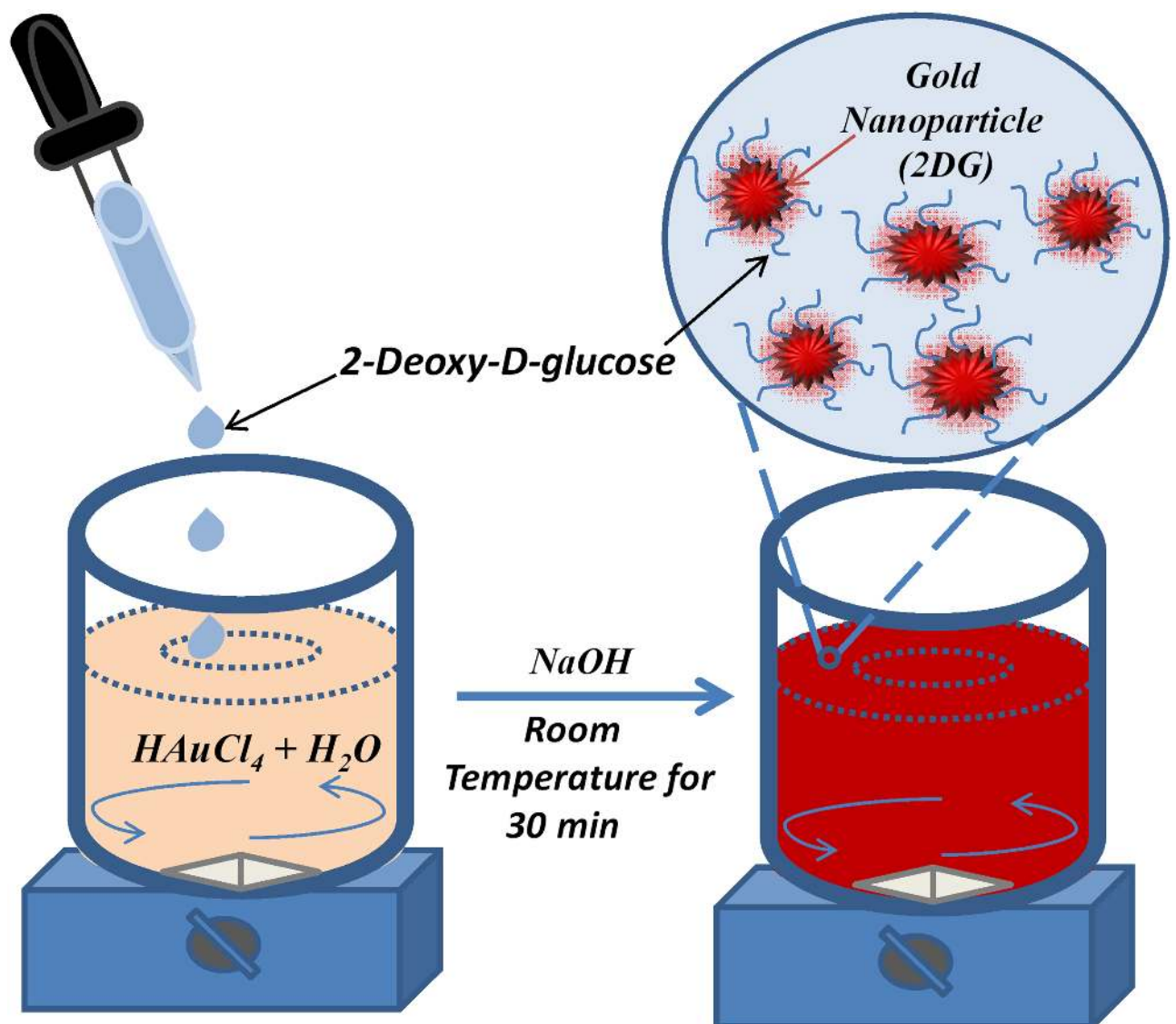


Fig 1. Flow chart of 2DG AuNP. Flow chart of synthesis of 2DG gold nanoparticle at room temperature method.

<https://doi.org/10.1371/journal.pone.0178202.g001>

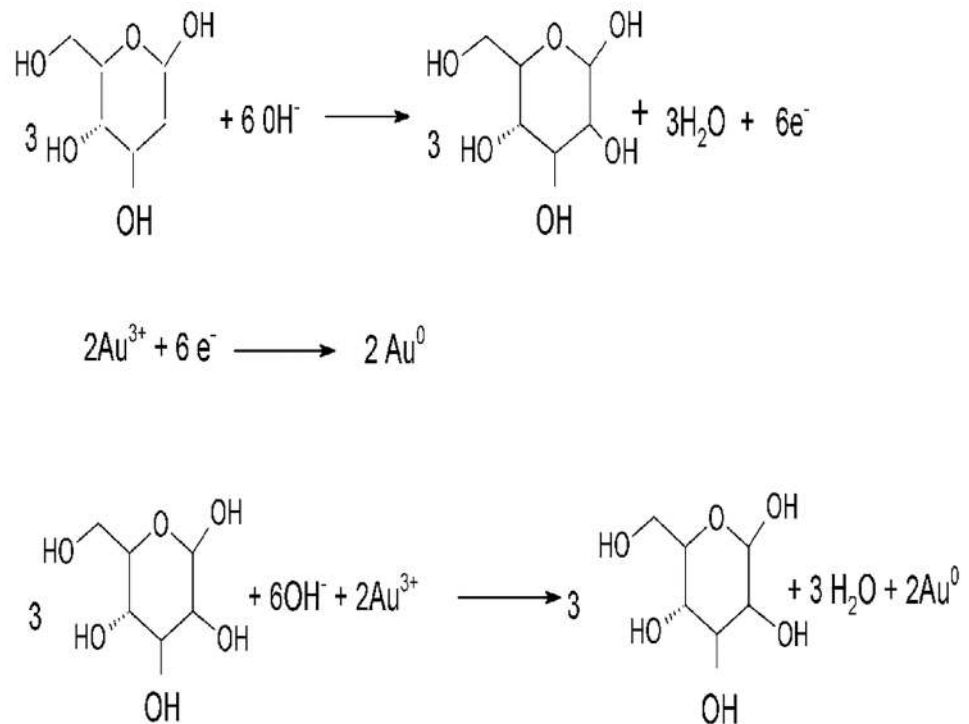


Fig 2. Chemical equation. The reduction reaction equation for the formation of Au nanoparticles.

<https://doi.org/10.1371/journal.pone.0178202.g002>

Characterization techniques. Gold nanoparticles stabilized with citrate, glucose and 2-deoxy-D-glucose are characterized by UV-Visible absorption spectroscopy (Shimadzu UV-1800). Confirmation of capping of the NPs has been done by FTIR (Shimadzu IR Prestige-21) analysis. Morphology and dimensions of the AuNps are studied through Dynamic light scattering (DLS; Malvern-Instrument) and Transmission electron microscopy (TEM; JEOL 2010 HRTEM). SEM-EDS (Carl Zeiss-SIGMA-Oxford Instrument) analysis is performed to verify the presence of gold content in AuNps. SERS study has been done using a micro-Raman setup (RAM HR, Jobin Yvon.).

HepG2, Hela cells and HCT 116 treatment with different capping agents of gold nanoparticles. Different cancer cell lines such as HepG2, HeLa and HCT 116 are treated with Glucose-AuNp, 2-deoxy-D-Glucose-AuNps and Citrate-AuNps at concentration ranging from 5 μM to 90 μM per ml of culture medium. The time of incubation of the cells with AuNps was 72 hrs. Throughout the experiments autoclaved AuNps without any centrifugation have been used. After 72 hrs the medium with AuNps was discarded and cells were washed thrice with phosphate buffer saline (PBS) to remove free Glu-AuNps, 2DG-AuNps and Citrate-AuNps.

MTT assay. To study the cell viability, MTT assay has been carried out for all the three different cell lines treated with the three differently capped AuNps viz. Gu-AuNps, 2DG-AuNps and Citrate-AuNps. Briefly Hep G2, HeLa and HCT 116 Cells are seeded in 96 well plate at a density of 10^4 and 10^6 cells per well prior to treatment with Glu-AuNps, 2DG-AuNps and Citrate-AuNps at various concentrations of the range 5 μM , 10 μM , 20 μM , 30 μM , 50 μM , 70 μM and 90 μM . The Glu-AuNp, 2DG-AuNps and Citrate-AuNps solution are used as positive control. 10 μl of MTT reagent (stock solution-5 mg/ml in PBS) is added in each well and incubated for 2.5 hrs in incubator (37°C, 5% CO₂ and 95% humidity). After careful removal of the medium from the well, 100 μl of DMSO is added to each well followed by measuring the

absorbance of Formazan at 595 nm by a BIO-RAD iMark™ micro plate reader. MTT assay has been performed in triplicate, Error bars are SEM (n = 8) for MTT assay one-way ANOVA has been done and $p < 0.05$ has been considered as the level of significance.

Results and discussion

UV-Visible spectroscopy of gold nanoparticles

Fig 3 represents the absorption spectrum of the three differently capped AuNps. The strong absorbance peaks observed at 540 nm, 525 nm and 520 nm for Glu-AuNps, 2DG-AuNps and Citrate-AuNps respectively, show the presence AuNps.

The absorbance maxima of the three respective AuNps are confirmed from earlier reports [42,43]. During citrate-AuNp synthesis, citrate acts as reducing (Au^{3+} to Au^0) as well as capping agent. In the case of Glu-AuNp synthesis, glucose acts as reducing (Au^{3+} to Au^0) as well as capping agents in alkaline aqueous environment due to addition of NaOH. Glucose is

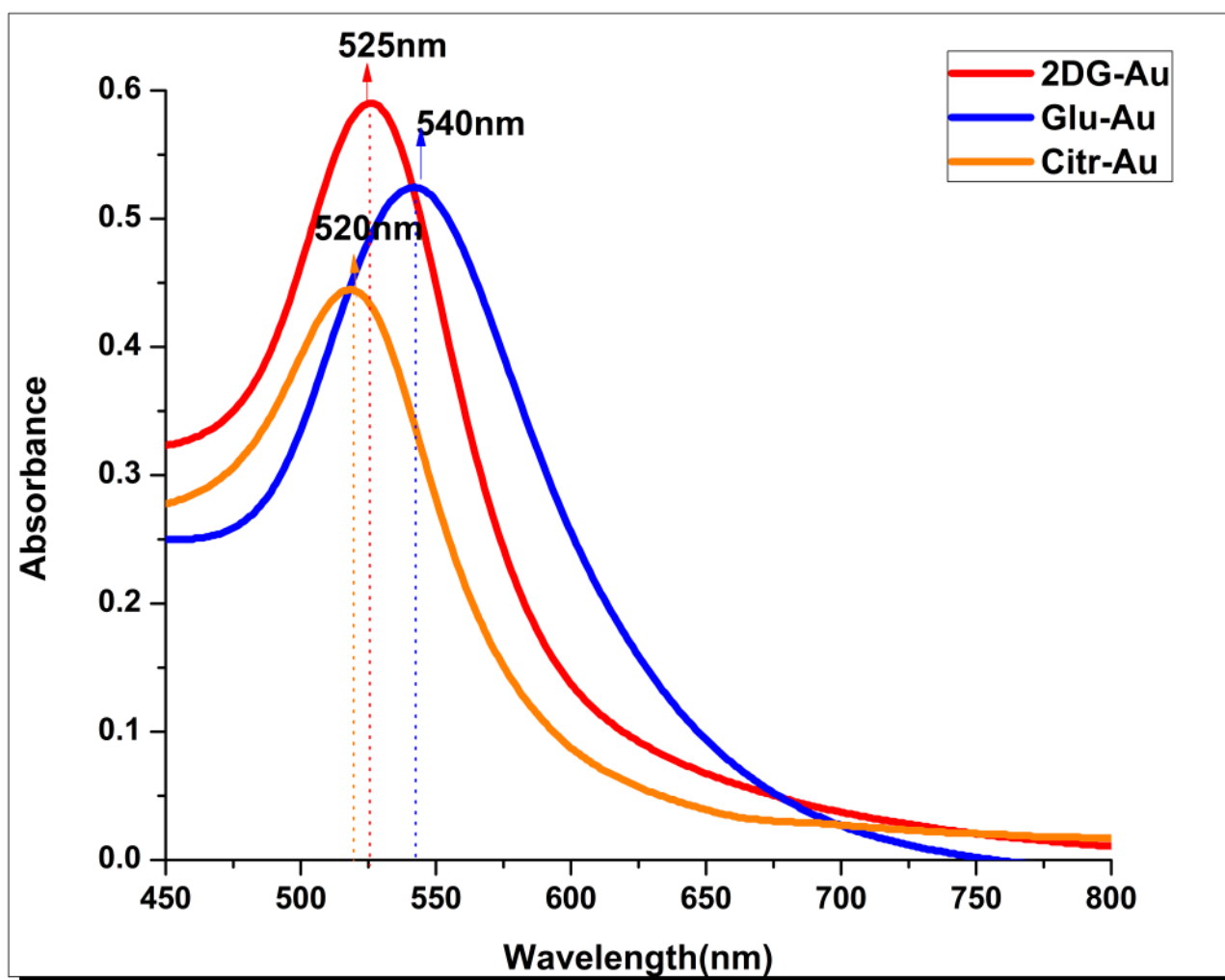


Fig 3. UV-visible absorption spectrum of AuNPs. A UV-visible absorption spectrum of glucose-AuNps showing SPR peak at 540 nm; **B** Citrate-AuNps showing SPR peak at 520 nm; **C** 2DG-AuNps showing SPR peak at 525 nm.

<https://doi.org/10.1371/journal.pone.0178202.g003>

bound to surface of nanogold by hydrogen bonding of hydroxyl (-OH) group and similar changes observed in case of 2-deoxy-D-Glucose.

FT-IR analysis of gold nanoparticles

Characterization of the particles using FT-IR shows the interaction between gold nanoparticles and the reducing agents (Fig 4).

FT-IR spectrum shows strong absorption peak at 3303 cm^{-1} (Fig 4A), manifesting the presence of β -D-glucose as an essential component of the Glu-AuNp. In addition, the absorption band of the -OH stretching undergoes a significant high frequency shift observed at 3303 cm^{-1} suggesting the intimate association between β -D-glucose and the surface of the Au nanoparticles [42]. FT-IR analysis of 2-deoxy-D-Glucose-AuNp exhibited a characteristic peak at 3318 cm^{-1} attributed to the stretching vibrations of -OH, which is assigned to -OH absorbed by gold nanoparticles (Fig 4B). The presence of characteristic bands in $1600\text{--}1000\text{ cm}^{-1}$ region corresponds to skeleton vibration of 2DG molecules. The hydrogen bond of chelate type appears as a wide degraded band in region $3500\text{--}3200\text{ cm}^{-1}$. The intensive bands in $1394\text{--}1018\text{ cm}^{-1}$ region observed in 2-deoxy-D-Glucose-AuNp correspond to deformation vibration of hydroxyl group. Well-defined peaks in the fingerprint region between $1000\text{--}1600\text{ cm}^{-1}$ confirms 2DG molecule adsorption on gold surface as these peaks corresponds to 2DG as established by earlier workers [44].

TEM analysis of gold nanoparticles

The size and shape of the gold nanoparticles using different capping agents as observed by TEM is shown in Fig 5.

TEM analysis show triangular shape of the glucose capped gold nanoparticles (Fig 5A and 5C) with narrow particle size-distribution of range $19.05\pm 1.13\text{ nm}$ and $\sigma = 0.15$. Furthermore, a few spherical gold nanoparticles also appeared in the image. ED pattern of these gold nanoparticles corresponded well to the crystalline planes of the face-centered-cubic (fcc) structured gold (Fig 5B), suggesting the crystalline nature of these Au nanoparticles. In addition, the multiple lattice fringes with an interplanar spacing of 2.36 \AA consistent with the interplanar distance of (111) plane can be observed clearly by using high-resolution TEM which also confirms the crystalline nature of the Glu-Au nanoparticles. In contrast to the triangular shape

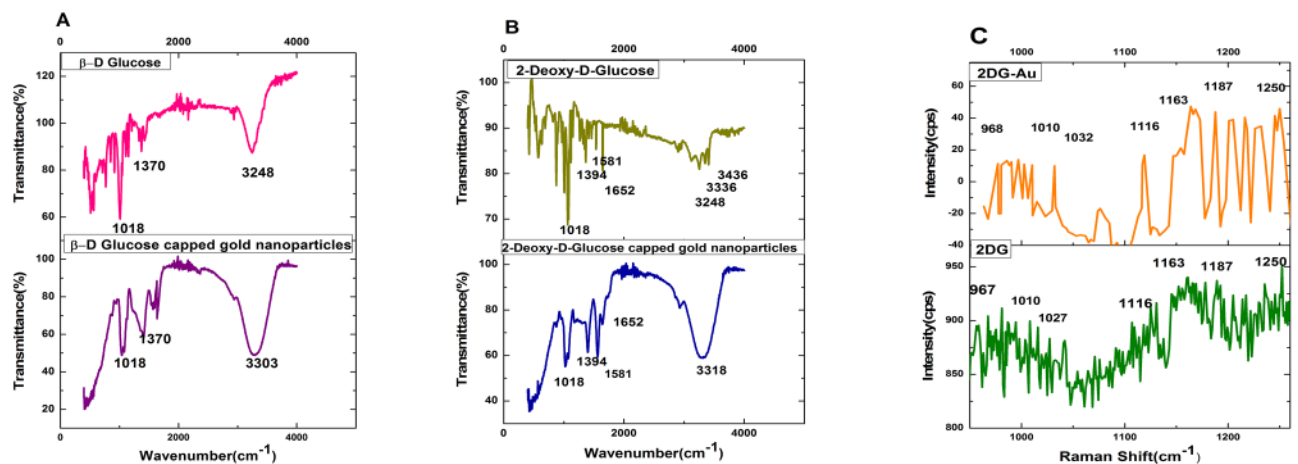


Fig 4. FTIR and SERS spectrum analysis. FTIR spectrum of (A) glucose and glucose-gold nanoparticles; (B) 2DG and 2DG-gold nanoparticles; C: SERS Raman spectra of 2DG-Au and Raman spectra of 2DG.

<https://doi.org/10.1371/journal.pone.0178202.g004>

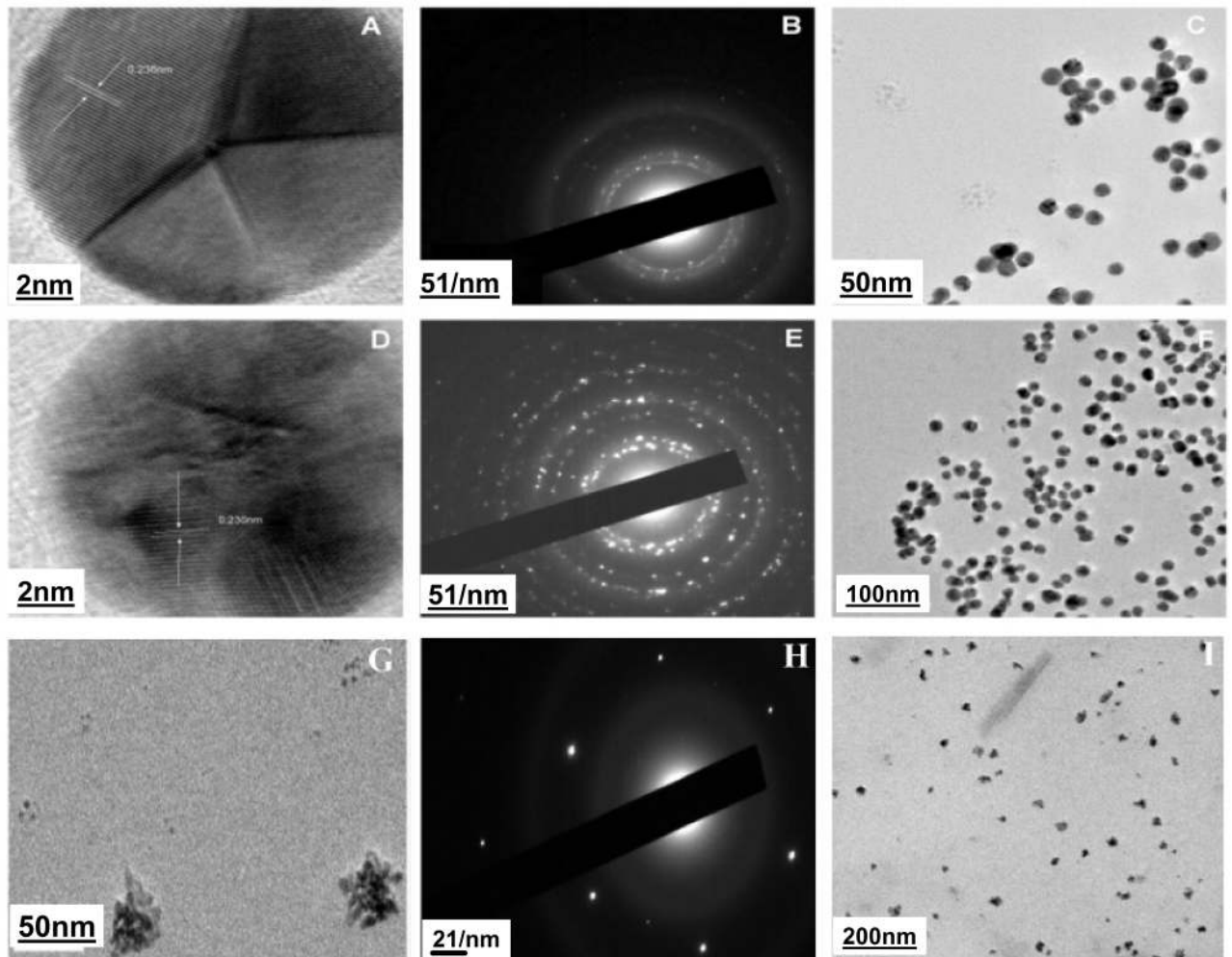


Fig 5. TEM analysis of AuNPs. **5A, 5C** High magnification TEM image of glucose capped gold nanoparticles showing FFT measurement using Image-J software; **5B** SAED pattern of glucose capped gold nanoparticles; **5D, 5F** High magnification TEM image of citrate-gold nanoparticles showing FFT measurement using Image J-software; **5E** SAED pattern of citrate—gold nanoparticles; **5 G, 5I** Shows the high magnification TEM image of 2-Deoxy-D-Glucose capped gold nanoparticles; **5 H** SAED pattern of 2DG-Capped gold nanoparticles.

<https://doi.org/10.1371/journal.pone.0178202.g005>

of the particles in Glu-AuNps, the citrate capped gold nanoparticles show spherical shape (Fig 5D and 5F) with majority of the particles having similar size of 14.87 nm ($\sigma = 0.15$) and inter planar spacing of 2.36 \AA . TEM image of citrate capped gold nanoparticles indicates a relatively high monodispersity of the Au nanoparticles formed in the system as compared to Glu-AuNps which confirms earlier reports [45]. Fig 5G–5I represent the TEM images of the 2DG-AuNps where ED pattern of these nanoparticles is shown in Fig 5H. Interestingly the 2DG-AuNps show urchin shape of the gold nanoparticles under TEM with a diameter of 21.51 nm, as observed by particle size analysis using DLS. Zeta potential value of 2DG-AuNp is -19.1 mv and has been observed to be stable for 8 months. The particle size distributions in the three differently capped AuNPs are shown in Fig 6.

Histogram plot in the Fig 6A represents the size distribution of Glu-AuNp, size distribution of the citrate-Au-nanoparticles is presented in the Fig 6B and 6C represents the size distribution of 2DG-AuNp, Presence of gold in the nanoparticles (Glu-AuNps and 2DG-AuNps) is confirmed by SEM-EDS analysis (Fig 7).

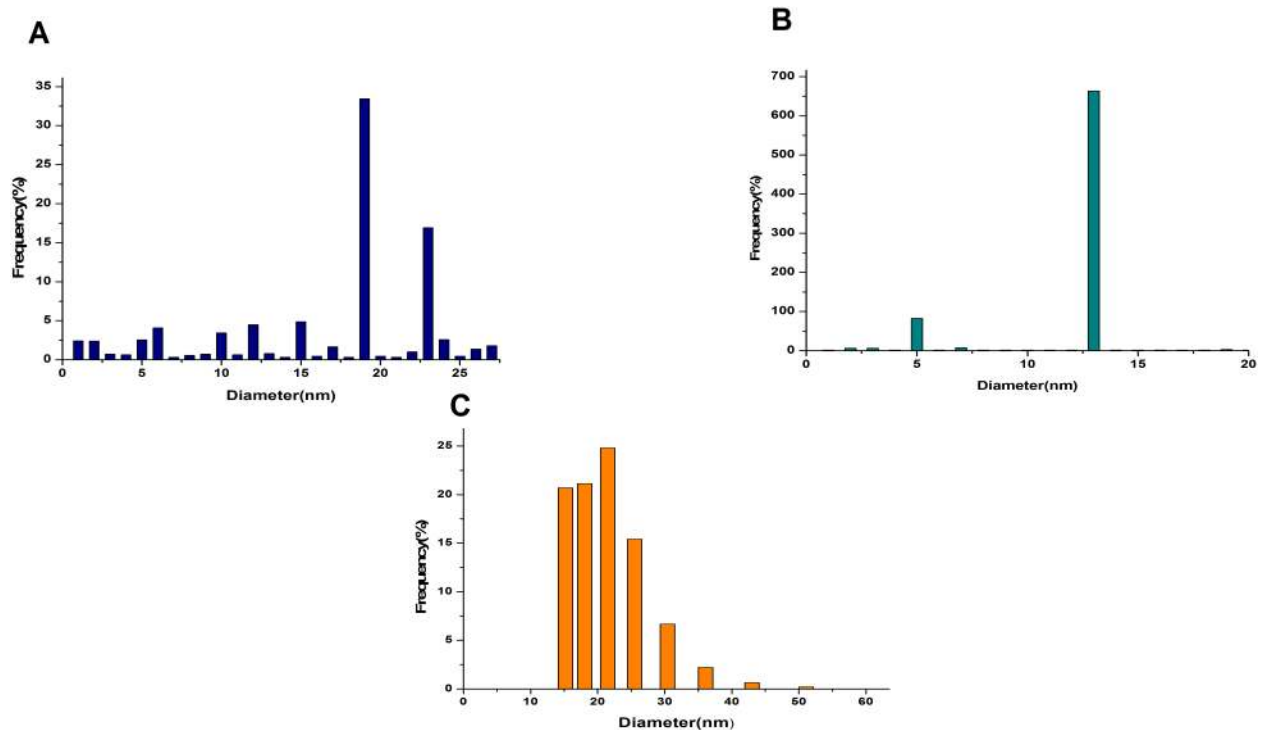


Fig 6. Size distribution measurement plot of AuNPs. Size distribution measurement curve of (A) glucose-gold nanoparticles; (B) citrate-gold nanoparticles; C Dynamic light scattering measurement of 2DG coated gold of size 21.51 nm.

<https://doi.org/10.1371/journal.pone.0178202.g006>

SERS analysis of gold nanoparticles

Surface-enhanced Raman scattering/spectroscopy (SERS), a vibrational spectroscopic method that provides information about molecular position, has raised a great interest as a sensitive technique for chemical and bioanalytical sensing and imaging [46–48]. Different shaped nanoparticle envisioned that these particles can be utilized to catalyse many other reactions, assembled to form super lattice structures, and serve as excellent SERS substrates [49]. When the molecules are adsorbed onto metallic surfaces with nanometer-scale roughness or onto metal

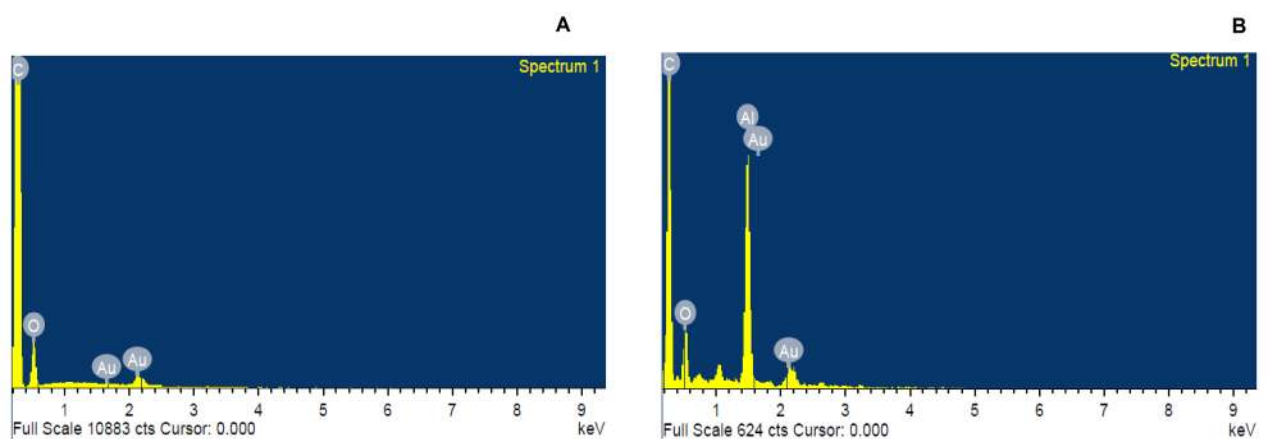


Fig 7. SEM-EDS spectrum of glucose-capped gold nanoparticles and 2DG-capped gold nanoparticles. SEM-EDS analysis of (A) glucose-capped gold nanoparticles; (B) 2DG-capped gold nanoparticles;

<https://doi.org/10.1371/journal.pone.0178202.g007>

nanoparticles, an enhancement in intensity of Raman scattering is observed [50,51]. Utilising this, there exists a plethora of work which has been performed to demonstrate SERS effects for different molecules, especially with different shaped nanoparticles [52,53]. Properties of the gold nanoparticles are dependent on their sizes, shapes, and crystallinity [54]. Gold nanoparticles have been used as effective surface-enhanced Raman spectroscopy (SERS) substrates for decades [55]. Our present study shows good SERS property of the 2DG-AuNp with 50 times increase in Raman signals (Fig 3C). The peak at 1032 cm^{-1} corresponds to C-H in plane bending and the Raman signal at 1163 cm^{-1} might appear due to C-H out of plane bending as a strong signal. Our observation finds support from earlier report [56]. At 967 cm^{-1} medium Raman signal observed is possibly due to C-O-C bond, while peak at 1116 cm^{-1} may be associated with orientation of C-O groups. Reports from earlier researchers also showed some bands at 1263 cm^{-1} assigned at complex modes of CH_2OH groups [57]. It is known well that in contrast to semiconductor or insulator nanomaterials, the optical properties of metal nanoparticles mainly depend on size and shape of the particles where, more sensitivity towards shape and less so to size is seen [58]. Recently it has been shown that the SERS enhancement factor generated from the gold nanoparticles increases as the size of nanoparticles increases [59]. However, the exact mechanism of SERS is still not clearly understood. Several groups have been working to explain the origin of SERS, and currently, the amplified electromagnetic (EM) field at the surface of the metal substrate is being considered as the main source of enhancement [60]. Recent studies have reported metal film over nanosphere surfaces as excellent candidates for experiments that were once impossible with more primitive SERS substrates [61]. Additionally, the colloidal nanostars showed the highest SERS enhancement factor while the nanospheres possessed the lowest SERS activity under different excitations [62]. Plasmonic gold nanostars offer a new platform for surface-enhanced-Raman-scattering (SERS). However, in conditions with the presence of organic surfactant on the nanoparticles, SERS characterization and application of nanostar in solution is a challenging factor in the field of SERS bioapplications [63]. Interestingly, FT-SERS studies showed that branched gold particles had stronger SERS activity relative to the nanobranched ones, which made these particles very attractive in the SERS applications [64]. In recent years, developments and applications of surface-enhanced Raman scattering (SERS) nanosensors and nanoreporters in biochemical monitoring, medical diagnostics, and therapy have been reported [65]. As gold nanoparticles that exhibit strong SERS properties are considered to be utilized for the development of biosensors and biocatalyst, the urchin like shaped gold nanoparticles (2DG-AuNps) synthesized by our group may be considered as more potent for biomedical applications because of their tunable SPR properties and excellent SERS enhancement ability. It has been shown earlier that such shaped nanoparticles are better candidates for applications in the optical imaging-based disease theranostics [66].

Effect of nanoparticles on the cell viability

Comparative analysis of the MTT assay data indicates that the three differently capped AuNps impart differential effects on survival of the three different types of cell lines (Fig 8A, 8B and 8C).

2DG-AuNp show negligible cell death in HCT 116 cells with no significant physiological state change of the cells, and manifested a survival of $\geq 80 \pm 0.70\%$ in all the concentration ranging from $5\text{--}90\ \mu\text{M}$ (Fig 8A). Results show that these nanoparticles are efficiently taken up by the cells and possess no cytotoxicity. Similar to this, Glu-AuNps also imparted no toxicity in HCT 116 cells and a $73 \pm 0.84\%$ cell viability has been observed in case of cells treated with $90\ \mu\text{M}$ (Fig 8B). However, in case of HCT 116 cells treated with citrate -AuNps a drastic drop

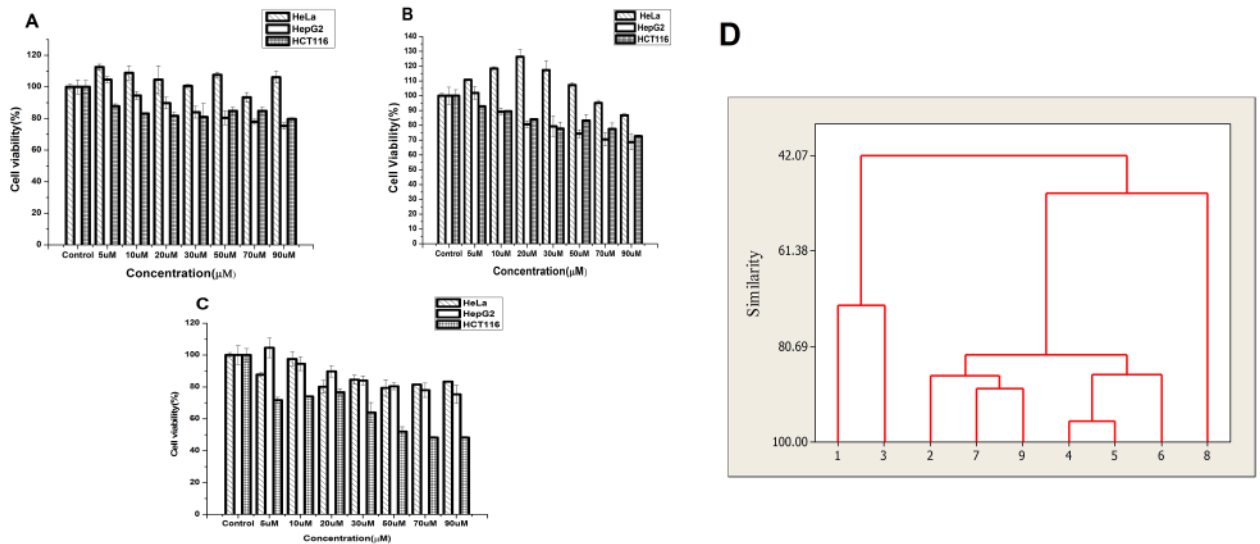


Fig 8. Cell viability plot and dendrogram plot. A Viability of HeLa cells, HepG2 cells and HCT 116 cells treated with 2-Deoxy-D-Glucose-gold nanoparticles; **B** Viability of HeLa cell line; HepG2 cell line and HCT116 cells treated with glucose capped gold nanoparticles; **C** Viability of HeLa cells, HepG2 cells and HCT 116 cells treated with citrate-gold nanoparticles. Standard deviation shown as error bar, $p < 0.05$. **D:** Dendrogram shows cell lines are aligned separately and grouped based on similarities in their cytotoxicity expression using a hierarchical clustering analysis technique. 1 represents 2DG-AuNp-Hela, 2: 2DG-AuNp-HepG2, 3: 2DG-AuNp-HCT116, 4: Glu-AuNp-Hela, 5: Glu-AuNp-HepG2, 6: Glu-AuNp-HCT116, 7: Citr-AuNp-Hela, 8: Citr-AuNp-HepG2, 9: Citr-AuNp-HCT116.

<https://doi.org/10.1371/journal.pone.0178202.g008>

of cell survival has been observed in cells treated with higher concentrations (50, 70, 90 μM) of the particles (Fig 8C). The present data indicating that higher concentration of citrate capped gold nanoparticles are toxic to HCT 116 cells, is in perfect harmony with the findings of some earlier researchers who reported similar observations and postulated that such toxicity might be associated with the acidic nature of citrate, the capping agent of the concerned nanoparticles [67]. Toxicity imparted by citrate –AuNp may also be due to the spherical shape of the particles supporting some earlier study who reported higher toxicity of gold nanospheres when compared to that of gold nanostars [68]. Interestingly, the present results reflect the potential of two of the synthesized nanoparticles to stimulate cell growth. Such stimulation of cell growth, however has been observed not only to be restricted to particular cell type but also depends upon the capping and shape of the nanoparticles. 5–50 μM concentrations of both Glu-AuNps and 2DG-AuNps have been observed to boost survival in Hela cells. In contrast to 90 μM Glu-AuNps showing $87 \pm 0.84\%$ viability of Hela cells (Fig 8B), same concentration of 2DG-AuNps manifested an increase in cell survival (Fig 8A). 2DG-AuNp-induced proliferative response of Hela cells has been reported by earlier researchers [69]. Citrate –AuNps showed no boosting in Hela cells but maintained $\geq 80 \pm 0.84\%$ viability of the cells when treated in the same concentration range (Fig 8C). HepG2 cells showed similar boost in cell growth when treated with 5 μM of all the three types of AuNps.

Fig 8D shows dendrogram of survivability of all the cell lines treated with the differently capped gold nanoparticles. Hierarchical clustering analysis manifest high degree of similarity between the 2DG-AuNp and Glu-AuNp treated Hela cells. While in case of HCT116 the differentially capped glucose AuNps also form a cluster (with similarity > 80.69), maximum similarity is observed between 2DG –Au Np and citrate- AuNps. In contrast, citrate-AuNp-HCT116 showing cytotoxicity is separated out from the clusters. Thus, results of the present investigation show among the three types of AuNps, while Glu-AuNps and 2DG-AuNps possess no cytotoxicity, 2DG-AuNp is most effective in maintaining survival in the three types of cancer

cells especially Hela cells. 2-deoxy-D- glucose has been reported earlier to be efficient in targeting tumor cells [70], which could be a perfect candidate for coupling to Au-nanoparticles to have biomedical applications, especially to target glucose-dependent cancer cells sparing the normal tissues and deliver the coupled drug to the site of interest[71,72]. Our present study portrays the possibility of 2-deoxy-D-glucose capped gold nanoparticles as a better candidate for theranostic application.

Acknowledgments

The authors thankfully acknowledge Prof. P.V. Satyam for the use of HRTEM facility at Institute of Physics, Bhubaneswar, India. The authors also acknowledge use of the facilities at Microtron center, Mangalore University.

Author Contributions

Conceptualization: SS YN AC.

Data curation: SS UD SKC MS AC YN.

Formal analysis: SS, UD SKC SM AC YN.

Funding acquisition: YN.

Investigation: SS UD SKC SM MS AC.

Methodology: SS AC YN.

Project administration: SS AC YN.

Resources: YN AC MS SD KDS.

Software: SS YN AC.

Supervision: YN AC KDS SD.

Validation: SS AC YN.

Visualization: SS UD SM AC YN.

Writing – original draft: SS AC YN.

Writing – review & editing: SS SKC AC YN.

References

1. Nicol JR, Dixon D, Coulter JA. Gold nanoparticle surface functionalization: a necessary requirement in the development of novel nanotherapeutics. *Nanomedicine*. 2015; 10:1315–1326. <https://doi.org/10.2217/nnm.14.219> PMID: 25955125
2. Haineld JF, Smilowitz HM, Conner MJ, Dilmanian FA, Selatkin DN. Gold nanoparticle imaging and radiotherapy of brain tumors in mice. *Nanomedicine*. 2013; 8(10):1601–1609. <https://doi.org/10.2217/nnm.12.165> PMID: 23265347
3. Boisseler E, Astruc D. Gold nanoparticles in nanomedicine: preparations, imaging, diagnostics, therapies and toxicity. *Chem Soc Rev*. 2009; 38:1759–1782. <https://doi.org/10.1039/b806051g> PMID: 19587967
4. Dykman L, Khlebtsov N. Gold nanoparticles in biomedical applications: Recent advances and perspectives. *Chem Soc Rev*. 2012; 41:2256–2282. <https://doi.org/10.1039/c1cs15166e> PMID: 22130549
5. Giasuddin ASM, Jheema KA, Haq AMM. Use of gold nanoparticles in diagnostics, surgery and medicine: A review. *J. Med. Biochem*. 2012; 5:56–60.
6. Zhang Q, Iwakuma N, Sharma P, Moudgil B, Wu C, McNeill J, et al. Gold nanoparticles as a contrast agent for in vivo tumor imaging with photoacoustic tomography. *Nanotechnology*. 2009; 20(39):395102 (8pp). <https://doi.org/10.1088/0957-4484/20/39/395102> PMID: 19726840

7. Mieszavoka AJ, Mulder WJM, Fayad ZA, Cormode DP. Multifunctional gold nanoparticles for diagnosis and therapy of disease. *Mol pharmaceutics*. 2013; 10:831–847.
8. Ramalingam M, Tiwari A, Ramakrishna S, Kobayashi H. *Integrated Biomaterials for Biomedical technology*. 2012; 440.
9. Mishra YK, Mohapatra S, Singhal R, Avasthi DK. Au-ZnO: A tunable localized surface plasmonic nanocomposite. *App.Phys.Lett*. 2008; 92:043107.
10. Polavarapu L, Mourdikoudis S, Santos IP, Juste JP. Nanocrystal engineering of noble metals and metal chalcogenides: controlling the morphology composition and crystallinity. *CrystEngComm*. 2015; 17:3727–3762.
11. Wahab R, Dwiverdi S, Khan F, Mistra YK, Hwang IH, Shin HS et al. Statistical analysis of gold nanoparticle-induced oxidative stress and apoptosis in myoblast (C₂C₁₂) cells. *Colloids and surfaces B: Biointerfaces*. 2014; 123:664–672. <https://doi.org/10.1016/j.colsurfb.2014.10.012> PMID: 25456994
12. Polavarapu L and Marzan LML. Growth and galvanic replacement of silver nanocubes in organic media. *Nanoscale*. 2013; 5:4355–4361. <https://doi.org/10.1039/c3nr01244a> PMID: 23571840
13. Mishra YK, Mohapatra S, Avasthi DK, Kabiraj D, Lalla NP, Pivin JC et al. Gold-Silica nanocomposites for the detection of human ovarian cancer cells: A preliminary study; *Nanotechnology*, 2007; 18,345606 (5pp).
14. Khan MS, Vishakante GD, Siddaramaiah H. Gold nanoparticles: a paradigm shift in biomedical applications. *Adv Colloid Interface Sci*. 2013; 199–200:44–58.
15. Pedrosa P, Vinhas R, Fernandes A, Baptista PV. Gold Nanotheranostics: Proof-of-concept or clinical tool?. *Nanomaterials*. 2015. 5:1853–1887. <https://doi.org/10.3390/nano5041853> PMID: 28347100
16. Hwang S, Nam J, Jung S, Song J, Doh H, Kim S. Goldnanoparticle-mediated photothermal therapy: current status and future perspective. *Nanomedicine*. 2014; 9(13):2003–2022. <https://doi.org/10.2217/nnm.14.147> PMID: 25343350
17. Wang L, Xu Y, Chen YC. Near-infrared light-mediated gold nanoplatforams for cancer theranostics. *Advances in nanotheranostics*. 2015; 6:3–52.
18. Nehl CL, Hafner JH. Shape-dependent Plasmon resonances of gold nanoparticles, *J Mater chem*. 2008. 18:2415–2419.
19. Huang X, Sayed MAE, Gold nanoparticles: optical properties and implementations in cancer diagnosis and photothermal therapy. *Journal of advanced research*. 2010. 1:13–18.
20. Bakr OM, Wunsch BH and Stellacci F. High-yield synthesis of multi branched urchin like gold nanoparticles. *Chem Mater*. 2006; 18:3297–3301.
21. Paterson S, Thompson SA, Gracie J, Wark AW and Rica RDL. Self-assembly of gold supraparticles with crystallographically aligned and strongly coupled nanoparticle building blocks for SERS and photothermal therapy. *chem.sci*. 2016; 6:232.
22. Shiohara A, Langer J, Polavarapu L and Marzan LML. Solution processed polydimethylsiloxane/gold star flexible substrates for plasmonic sensing. *Nanoscale*. 2014; 6:9817–9823. <https://doi.org/10.1039/c4nr02648a> PMID: 25027634
23. Zhang X. Gold nanoparticles: Recent advances in the biomedical applications. *Cell Biochem Biophys*. 2015; 72:771–775. <https://doi.org/10.1007/s12013-015-0529-4> PMID: 25663504
24. Cabuzu D, Cirja A, Puiu R, Grumezescu AM. Biomedical applications of gold nanoparticles. *Curr. Top. Med. Chem*. 2016; 15(16):1605–1613.
25. Maruyama T, Fujimoto Y, Maekawa T. Synthesis of gold nanoparticles using various amino acids. *Adv. Colloid Interface Sci*. 2015; 447:254–257.
26. Vigderman L, Zubarev ER. Therapeutic platforms based on gold nanoparticles and their covalent conjugates with drug molecules. *Adv. Drug Deliv. Rev*. 2013; 65:663–676. <https://doi.org/10.1016/j.addr.2012.05.004> PMID: 22613038
27. Simons AL, Ahmad IM, Mattson DM, Dornfeld KJ, Spitz DR. 2-deoxy-D-glucose combined with cisplatin enhances cytotoxicity via neck cancer cells. *Cancer Res*. 2007; 67(7): 3364–3370. <https://doi.org/10.1158/0008-5472.CAN-06-3717> PMID: 17409446
28. Kurtoglu M, Gao N, Shang J, Maher JC, Lehrman MA, Wangpaichitr M et al. Under normoxia, 2-deoxy-D-glucose elicits cell death in select tumor types not by inhibition of glycolysis but by interfering with N-linked glycosylation. *Mol Cancer Ther*. 2007; 6(1):3049–3058.
29. Zhong D, Liu X, Schafer-hales K, Marcus AI, Khuri FR, Sun SY et al. 2-Deoxyglucose induces akt phosphorylation via a mechanism independent of LKB1/AMP-activated protein kinase signaling activation or glycolysis inhibition. *Mol Cancer Ther*. 2008; 7(4): 809–817. <https://doi.org/10.1158/1535-7163.MCT-07-0559> PMID: 18413794

30. Kung HT, Hwang ES. 2-deoxyglucose: An anticancer and antiviral therapeutic, but not anymore a low glucose mimetic. *Life Sci.* 2006; 78(12):1392–1399. <https://doi.org/10.1016/j.lfs.2005.07.001> PMID: [16111712](https://pubmed.ncbi.nlm.nih.gov/16111712/)
31. Zhang D, Li J, Wang F, Hu J, Wang S, Sun Y. 2-Deoxy-D-Glucose targeting of glucose metabolism in cancer cells as a potential therapy. *Cancer Lett.* 2014; 355(2):176–183. <https://doi.org/10.1016/j.canlet.2014.09.003> PMID: [25218591](https://pubmed.ncbi.nlm.nih.gov/25218591/)
32. Feng G, Kong B, Chen XJ. Enhancing multimodality functional and molecular imaging using glucose-coated gold nanoparticles. *Clin Radiol.* 2014; 69(11):1105–1111. <https://doi.org/10.1016/j.crad.2014.05.112> PMID: [25023059](https://pubmed.ncbi.nlm.nih.gov/25023059/)
33. Li J, Chaudhary A, Chmura SJ, Pelizzari C, Tijana R, Wietholt C et al. A novel functional CT contrast agent for molecular imaging of cancer. *Phys.Med.Biol.*2010; 55:4389–4397. <https://doi.org/10.1088/0031-9155/55/15/013> PMID: [20647599](https://pubmed.ncbi.nlm.nih.gov/20647599/)
34. Curry T, Kopelman R, Shilo M and Popovtzer R, Multifunctional theranostic gold nanoparticles for targeted CT imaging and photothermal therapy. *Contrast Media Mol. Imaging.*2014; 9:53–61. <https://doi.org/10.1002/cmml.1563> PMID: [24470294](https://pubmed.ncbi.nlm.nih.gov/24470294/)
35. Shilo M, Reuveni T, Motiei M, Popovtzer R, Nanoparticles as computed tomography contrast agents: current states and future perspectives. *Nanomedicine.* 2012; 7(2):257–269. <https://doi.org/10.2217/nnm.11.190> PMID: [22339135](https://pubmed.ncbi.nlm.nih.gov/22339135/)
36. Cole LE, Ross RD, Tilley JMR, Gogola TV, Kroeder R. Gold nanoparticles as contrast agents in x-ray imaging and computed tomography. *Nanomedicine.* 2015; 10(2):321–341. <https://doi.org/10.2217/nnm.14.171> PMID: [25600973](https://pubmed.ncbi.nlm.nih.gov/25600973/)
37. Meir R, Shamalov K, Betzer O, Motiei M, Horwitz-fried M, Yehuda R et al. Nanomedicine for cancer immunotherapy: Tracking cancer-specific t-cells in vivo with gold nanoparticles and CT imaging, *ACS Nano.* 2015; 9(6): 6363–6372. <https://doi.org/10.1021/acs.nano.5b01939> PMID: [26039633](https://pubmed.ncbi.nlm.nih.gov/26039633/)
38. Hu C, Niestroj M, Yuan D, Chang S, Chen J. Treating cancer stem cells and cancer metastasis using glucose-coated gold nanoparticles. *Int J Nanomedicine.* 2015; 10:2065–2077. <https://doi.org/10.2147/IJN.S72144> PMID: [25844037](https://pubmed.ncbi.nlm.nih.gov/25844037/)
39. Roa W, Xiong Y, Chen J, Yang X, Kong B, Wilson J et al. Pharmacokinetic and toxicological evaluation of multi-functional thiol-6-fluoro-6-deoxy-D-glucose gold nanoparticles in vivo. *Nanotechnology.* 2012; 23:375101. <https://doi.org/10.1088/0957-4484/23/37/375101> PMID: [22922305](https://pubmed.ncbi.nlm.nih.gov/22922305/)
40. Gorin F, Harley W, Schnier J, Lyeth B, Jue T. Perinecrotic glioma proliferation intracerebral tumor xenograft. *Acta Neuropathol.* 2004; 107(3):235–244. <https://doi.org/10.1007/s00401-003-0803-1> PMID: [14712400](https://pubmed.ncbi.nlm.nih.gov/14712400/)
41. Jiang X, Xin H, Ren Q, Gu J, Zhv L, Du F et al. Nanoparticles of 2-deoxy-d-glucose functionalized poly(ethylene glycol)-co-poly(trimethylene carbonate) for dual-targeted drug delivery in glioma treatment. *Biomedicals.* 2014; 35:518–529.
42. Liu J, Qin G, Raveendran P and, Facile YI. “Green” Synthesis, characterization, and catalytic Function of β -D-glucose Stabilized Au Nanocrystals, *A European Journal.*2009; 12:2131–2138.
43. Turkevich J, Stevenson PC, Hillier J. A study of the nucleation and growth processes in the synthesis of colloidal gold. *Discuss Faraday Sol.*1951; 11:55–75.
44. Maharramev AM, Ramazanov MA, Ahadova AI, Kloor M, Kopitz J, Doeberitz VK M, et al. Preparation of 2-deoxy-D-Glucose coated spio nanoparticles and characterization of their Physical, Chemical and Biological properties. *Dig J Nanomater Biostruct.* 2014; 9:1461–1469.
45. Chen F, Wang Y, Ma J and Yang G. A biocompatible synthesis of gold nanoparticles by Tris(hydroxymethyl)aminomethane. *Nanoscale Research Letters* 2014; 9:220. <https://doi.org/10.1186/1556-276X-9-220> PMID: [25006333](https://pubmed.ncbi.nlm.nih.gov/25006333/)
46. Fleischmann M, Hendra PJ, McQuillan AJ. Raman spectra of pyridine adsorbed at a silver electrode. *Chem.Phys.Lett.*1974; 26:163–166.
47. Moskovits M. Surface-enhanced spectroscopy. *Rev. Mod. Phys.*1985; 57:No.3,part I.
48. Haynes CL, McFarland AD, VanDuyne RP, Surface enhanced raman spectroscopy. *Anal.Chem.*2005; 77(17):338A–246A.
49. Tsao YC, Rej S, Chiu CY and Michael H. Aqueous phase synthesis of Au-Ag core- shell nanocrystals with tunable shapes and their optical and catalytic properties, *J.Am.Chem.Soc.*2014; 136:396–404. <https://doi.org/10.1021/ja410663g> PMID: [24341355](https://pubmed.ncbi.nlm.nih.gov/24341355/)
50. Kneipp K, Moskovits M, and Kneipp H. *Surface-Enhanced Raman Scattering.* Springer, Berlin.2006.
51. Champion A, Kambhampati P. surface-enhanced Raman scattering. *Chem. Soe. Rev.* 1988; 27:241–250.

52. Jackson JB and Halas NJ. Optical spectroscopy and computational methods in biology and medicine. *Proc Natl Acad Sci USA*. 2004; 101:17930–17935.
53. Bhaskar S, Tian F, Stoeger T, Kreyling W, De la Fuente JM, Grazu V, Borm P et al. Multifunctional nanocarriers for diagnostics, drug delivery and targeted treatment across blood-brain barrier: perspectives on tracking and neuroimaging. *Part Fibre Toxicol*. 2010; 7,3. <https://doi.org/10.1186/1743-8977-7-3> PMID: [20199661](https://pubmed.ncbi.nlm.nih.gov/20199661/)
54. Zhao P, Li N, Astruc D. State of the art in gold nanoparticle synthesis, *Coord. Chem. Rev.* 2013; 257(3–4):638–665.
55. Nie S and Emory SR. Probing single molecules and single nanoparticles by surface-enhanced Raman scattering. *Science*. 1997; 275(5303):1102–1106. PMID: [9027306](https://pubmed.ncbi.nlm.nih.gov/9027306/)
56. Quester K, Borja MA, Nestor ARV, Antonia M, Lopez C, Longoria EC. SERS Properties of different sized and shaped gold nanoparticles biosynthesized under different environmental conditions by *Neurospora crassa* Extract. *PLoS ONE*. 2013; 8(10):e77486. <https://doi.org/10.1371/journal.pone.0077486> PMID: [24130891](https://pubmed.ncbi.nlm.nih.gov/24130891/)
57. Wen ZQ, Barron LD, Hecht L. Vibrational Raman optical activity of monosaccharides, *J. Am Chem. Soc.* 1993; 115:285–292.
58. Zhang JZ. Optical properties of metal Nanomaterial. 2009; 205–235.
59. Hong S and Li X. Optimal size of gold nanoparticles for surface-enhanced raman spectroscopy under different conditions, *Journal of nanomaterials*. 2013; 790323:9.
60. Stiles PL, Dieringer JA, Shah NC, Van Duyer RP. Surface-Enhanced Raman spectroscopy, *Ann. Rev. Anal. Chem.* 2008; 1:601–626.
61. Li M, Cushing SK, Zhang J, Lankford J, Aguilar ZP, Ma D, Wu N. Shape-dependent surface-enhanced Raman scattering in gold–Raman-probe-silica sandwiched nanoparticles for biocompatible applications. *Nanotechnology*. 2012; 23:115501. <https://doi.org/10.1088/0957-4484/23/11/115501> PMID: [22383452](https://pubmed.ncbi.nlm.nih.gov/22383452/)
62. Yuan H, Fales AM, Khoury CG, Liu J, Dinh TV. Spectral characterization and intracellular detection of surface-enhanced Raman scattering (SERS)-Encoded plasmonic gold nanostars. *J. Raman Spectrosc.* 2013; 44(2):234–239.
63. Zou X, Ying E, Dong S. Seed-mediated synthesis of branched gold nanoparticles with the assistance of citrate and their surface-enhanced raman scattering properties. *Nanotechnology*. 2006; 17:4758–4764. <https://doi.org/10.1088/0957-4484/17/18/038> PMID: [21727609](https://pubmed.ncbi.nlm.nih.gov/21727609/)
64. Dinh TV, Liu Y, Fales AM, Ngo H, Wang HN, Register JK, et al. SERS nanosensors and nanoreporters: Golden opportunities in biomedical application. *Nanomedicine and nanobiotechnology*. 2015; 7(1):17–33. <https://doi.org/10.1002/wnan.1283> PMID: [25316579](https://pubmed.ncbi.nlm.nih.gov/25316579/)
65. Cai W, Gao T, Hong H and Sun J, Applications of gold nanoparticles in cancer in nanotechnology. *Nanotechnol Sci Appl*; 2008:1.
66. Lu L, Ai K, Ozaki Y, Environmentally friendly synthesis of highly monodisperse biocompatible gold nanoparticles with urchin-like shape. *Langmuir*. 2008; 24:1058–1063.
67. Vijayakumar S, Ganeasan S. *In vitro* cytotoxicity assay on gold nanoparticles with different stabilizing agents, *J Nanomater*. 2012; Article ID:734398,9 pages.
68. Favi PM, Gao M, Johana L, Arango S, Ospina SP, Morales M, et al. Shape and surface effects on the cytotoxicity of nanoparticles: Gold nanospheres verses gold nanostars, *J Biomed Mater Res*. 2015; 103(1):3449–3462.
69. Anderson KM, Tsui P, Guinan P, Rubenstein M. The proliferative response of HeLa cells to 2-deoxy-D-glucose under hypoxic or anoxic conditions: an analogue for studying some properties of invivo solid cancers. *Anticancer Res*. 2006; 26(6B):4155–4162. PMID: [17201127](https://pubmed.ncbi.nlm.nih.gov/17201127/)
70. Xiong F, Zhu Z, Xing C, Hua X, Sha X, Zhang Y, Gu N. Preparation characterization of 2-deoxy-D-glucose functionalized dimercaptosuccinic acid-coated maghemite nanoparticles for targeting tumor cells. *Pharm res*. 2012; 29: 1087–1097. <https://doi.org/10.1007/s11095-011-0653-9> PMID: [22173782](https://pubmed.ncbi.nlm.nih.gov/22173782/)
71. Dwarakanath BS, Cytotoxicity, radiosensitization and Chemosensitization of tumor cells by 2-deoxy-D-glucose in-vitro. *J Can Res Ther*. 2009; 5:S27–S31.
72. Aydogan B, Li J, Rajh T, Chaudhary A, Chmura SJ, Pelizzari C et al., AuNP-DG: Deoxyglucose-Labeled Gold Nanoparticles as X-ray computed Tomography contrast agents for cancer imaging, *Mol Imaging Biol*, 12,463–467. <https://doi.org/10.1007/s11307-010-0299-8> PMID: [20237857](https://pubmed.ncbi.nlm.nih.gov/20237857/)